JACS
JOURNAL OF THE AMERICAN CHEMICAL SOCIETY

ARTICLE

pubs.acs.org/JACS

Intermolecular Migratory Insertion of Unactivated Olefins into Palladium−Nitrogen Bonds. Steric and Electronic Effects on the Rate of Migratory Insertion

Patrick S. Hanley and John F. Hartwig*

Department of Chemistry, University of Illinois at Urbana−Champaign, 600 South Mathews Avenue, Urbana, Illinois 61801, United States

Supporting Information

ABSTRACT: We report a detailed examination of the effect of the steric and electronic properties of the ancillary ligand and the alkene reactant on the rate of migratory insertion of unactivated alkenes into the palladium−nitrogen bond of isolated palladium amido complexes. A series of THF-bound and THF-free amidopalladium complexes ligated by cyclometalated benzylphosphine ligands possessing varied steric and electronic properties were synthesized. The THF-free complexes react with ethylene at −50 °C to form olefin-amido complexes that were observed directly and that undergo migratory insertion, followed by β-hydride elimination to generate enamine products. The effect of the steric properties of the ancillary ligand on the binding of the alkene and the rate of migratory insertion were evaluated individually. The relative binding affinity of ethylene vs THF is larger for the less sterically hindered complex than for the more hindered complex, but the less hindered complex undergoes the insertion of ethylene more slowly than does the more hindered complex. These two changes in relative equilibrium and rate constants cause the rates of reaction of ethylene with the two THF-ligated species having different steric properties to be similar to each other. Reactions of the complexes containing electronically varied ancillary ligands showed that the more electron-poor complexes underwent the migratory insertion step faster than the more electron-rich complexes. Reactions of a THF-ligated palladium-amide with substituted vinylarenes showed that electron-poor vinylarenes reacted with the amido complex slightly faster than electron-rich vinylarenes. Separation of the energetics of binding and insertion indicate that the complex of an electron-rich vinylarene is more stable in this system than the complex of a more electron-poor vinylarene but that the insertion step of the bound, electron-rich vinylarene is slower than the insertion step with the bound, electron-poor vinylarene.

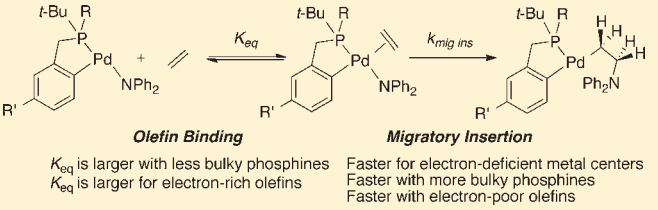

INTRODUCTION

Migratory insertions of alkenes are among the most documented organometallic transformations. This class of reaction is a common step in numerous catalytic processes, including the polymerization of alkenes,[1−4] the hydroarylation of alkenes,[5−9] the difunctionalization of alkenes,[10−13] and the olefination of aryl halides, commonly termed the Mizoroki-Heck reaction.[14−17] Many organometallic complexes react to form new C−C and C−H bonds by the transfer of a transition metal hydrocarbyl or hydride group to a coordinated olefin.[18] However, the transfer of an amido group from an isolated transition metal amido complex to an olefin to generate a new C−N bond is much less established.

Many of the prior reactions of alkenes with isolated amido complexes have required activated alkenes. Milstein, Casalnuovo, and co-workers reported an iridium(III) arylamido complex that inserts norbornene, but reactions with less-strained olefins were not observed.[19] Trogler et al. reported the transfer of an amido ligand from an isolated platinum-amido complex to acrylonitrile, but this reaction most likely occurs by direct nucleophilic attack of the nitrogen of the amide on the electrophilic acrylonitrile.[20] Boncella et al. reported the reaction of a palladium amide with dimethylacetylene dicarboxylate, but alkenes and unactivated alkynes did not react.[21]

Less-activated alkenes undergo intramolecular insertion into amido complexes characterized in situ, and recent catalytic hydroaminations of secondary aminoalkenes catalyzed by group IV transition metal complexes are thought to occur by alkene insertion into the metal−amide bond.[22−24] For example, Marks et al. reported the intramolecular insertion of an olefin into a lanthanide-amide generated in situ,[25] and Hultzsch has reported the hydroamination of secondary aminoalkenes catalyzed by cationic ziroconcene and titanocene complexes.[26] More recently, Wolfe reported the intramolecular insertion of an alkene into a palladium-amido complex generated and characterized in situ.[27,28]

The authors' group has reported the isolation and full characterization of a series of isolated rhodium(I) amido complexes that react intermolecularly with unactivated alkenes and vinylarenes to generate imine products.[29] Potential pathways for the transfer of the amido group were investigated by a series of

Received: June 20, 2011
Published: August 04, 2011

dx.doi.org/10.1021/ja205722f | J. Am. Chem. Soc. 2011, 133, 15661–15673

Scheme 1. Reactions of THF-Ligated Palladium-Amides 2a−e with Ethylene and Octene

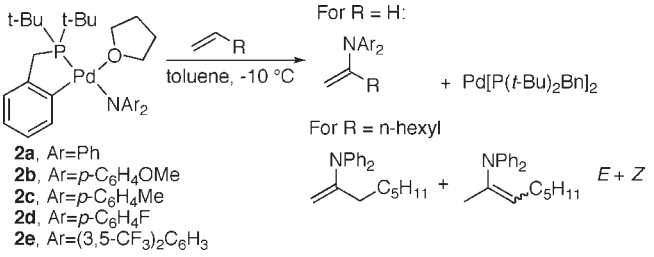

mechanistic experiments. All the mechanistic data were consistent with a pathway initiated by coordination of the alkene to the metal center, migratory insertion of the olefin into the rhodium-amido bond, and β-hydrogen elimination from the resulting aminoalkene complex.

In addition, migratory insertion has been proposed to occur during several classes of palladium-catalyzed aminations of alkenes, including carboaminations,[30−34] oxidative aminations,[35−37] aminoacetoxylations,[38] diaminations,[39] chloro-aminations,[40] and hetero-Heck type transformations.[41] Stereochemical evidence for *syn*-aminopalladation by migratory insertion has been obtained during studies of some of these systems. For example, Stahl and co-workers have shown that a complex generated from Pd(OAc)$_2$ and pyridine catalyzes the oxidative cyclization of deuterium-labeled aminoalkenes to generate products from *syn*-aminopalladation,[42] and Wolfe and co-workers have shown that the stereochemical outcome of alkene carboaminations they developed is consistent with a mechanism involving the migratory insertion of an alkene into a metal−amide bond.[27] Although data have been reported that imply that alkenes insert into palladium−nitrogen bonds during catalytic reactions, discrete complexes involved in palladium-catalyzed olefin aminations, other than those studied in the current work, have not been isolated. Studies aimed at revealing steric and electronic effects on the insertions of alkenes into the Pd−N bonds of phosphine-ligated intermediates in palladium-catalyzed carboamination reactions were stated to reveal the effect of these properties on the rate of ligand dissociation, rather than the rate of the C−N bond-forming migratory insertion step.[28]

We recently reported the intermolecular insertion of ethylene and octene into the Pd−N bonds of discrete, isolated palladium diarylamido complexes to form enamine products.[43] Stable, THF-bound Pd-amido complexes ligated by a cyclometalated benzylphosphine ligand reacted with ethylene to form *N*-vinyl diarylamine products over 2 h at −10 °C (Scheme 1). The stereochemical outcome of the reaction of *trans*-ethylene-d_2 implied that the reaction occurred by insertion of the alkene into the metal-amido bond. Reactions of ethylene with a series of amido complexes containing different substituents on the diarylamide showed that the palladium-amido complexes containing more electron-donating amido groups reacted with alkenes faster than those containing less electron-donating amido groups. During these studies, a diarylamido complex lacking the THF ligand also was isolated, and this unsaturated complex reacted with ethylene at −50 °C in toluene-d_8 to form vinyl diphenylamine in high yield. Moreover, this amido complex lacking coordinated THF reacted at low temperatures with ^{13}C-labeled ethylene to form a species proposed to be the amido ethylene precursor to the actual migratory insertion process.

These studies on the reactions of alkenes with discrete amidopalladium complexes set the stage for a detailed analysis of the effect of the steric and electronic properties of the ancillary ligand and of the alkene on the rate of insertion. Such effects could then be compared to those known for insertions of alkenes into metal−alkyl complexes, and the effects of the differences in bond polarity, bond strength, and the presence or absence of an electron pair could be determined.

To this end, we report the synthesis of a series of amidopalladium complexes possessing varied steric and electronic properties and studies on the reactions of these complexes with olefins that reveal detailed information on the insertion process. This series of complexes reacts with ethylene in high yield through a directly observed ethylene amido complex, and they react with vinylarenes having systematically varied electronic properties. This combination of experiments creates a map of the effects of the steric and electronic properties of the system on this new class of alkene insertion reaction. Some of the effects on the rates of these reactions are distinct from those for insertions into metal−carbon bonds but other effects parallel those observed for insertions into metal−carbon bonds, despite the significant differences in the properties of the reactive metal−ligand bond.

RESULTS AND DISCUSSION

Synthesis and Characterization of Palladium-Diarylamido Complexes. To prepare a series of amidopalladium complexes that undergo migratory insertion reactions with alkenes, we previously targeted complexes that are isoelectronic with the rhodium amides we had shown to undergo intermolecular alkene insertion reactions. To encourage the isolation of monomeric complexes and to discourage C−N bond-forming reductive elimination from unsaturated arylpalladium-amido complexes, cyclometalated species generated from bulky, chelating P−C ligands were synthesized. The synthesis of these complexes was accomplished by a two-step procedure involving initial formation of a dimeric complex with bridging chloride ligands from the reaction of Pd(OAc)$_2$ with di-*tert*-butylbenzylphosphine and subsequent addition of LiCl in methanol. Reaction of the dimeric chloride complexes with potassium diarylamides generated the diarylamido complexes **2a**−**2e** shown in Scheme 1. The characterization of these complexes was reported previously in communication form.[43]

To map the effects of the electronic properties of the ligands on the rates of these migratory insertions of alkenes into the Pd−N bonds of the diarylamido complexes, we sought to prepare a series of complexes bearing phosphine ligands with varied steric and electronic properties. Dimeric, cyclometalated palladium-chloride complexes **1a**, **1g**, and **1h** containing different substituents on the cyclometalated benzylphosphine ligand were prepared from the parent benzyl di-*tert*-butylphosphine and from benzyl di-*tert*-butylphosphines containing *meta*-trifluoromethyl and *meta*-methoxy substiutents on the aryl ring. The palladium-diphenylamido complexes were synthesized from the isolated chloride dimers by the addition of KNPh$_2$ (Scheme 2).

Attempts to prepare the analogous amido complexes containing less hindered ligands led to complicated mixtures of products. Dimeric, cyclometalated palladium chloride complexes containing isopropyl, phenyl, and cyclohexyl groups were synthesized, but attempts to prepare monomeric palladium-diarylamido

Scheme 2. Synthesis of THF Ligated Palladium-Amides 2a, 2f–h, and THF-Free Pd Amides 3a, 3f–h, and 4a, 4f–h

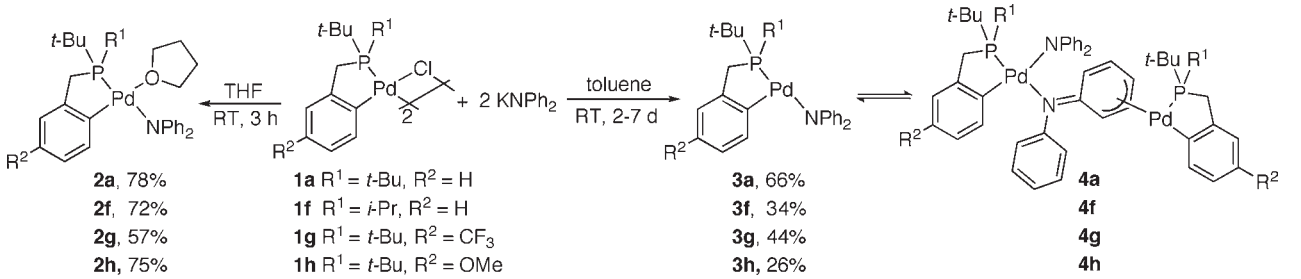

2a, 78% **1a** R^1 = *t*-Bu, R^2 = H **3a**, 66% **4a**
2f, 72% **1f** R^1 = *i*-Pr, R^2 = H **3f**, 34% **4f**
2g, 57% **1g** R^1 = *t*-Bu, R^2 = CF_3 **3g**, 44% **4g**
2h, 75% **1h** R^1 = *t*-Bu, R^2 = OMe **3h**, 26% **4h**

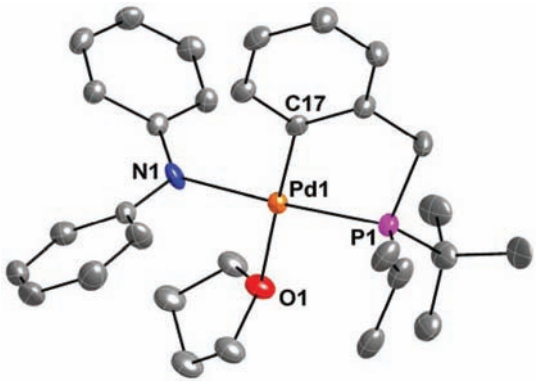

Figure 1. ORTEP diagram of **2f** with 35% probability ellipsoids. Hydrogen atoms are omitted for clarity.

Table 1. Selected Bond Distances (Å) and Angles (degrees) in Palladium-Amides 2a and 2f

entry	parameter[a]	2a	2f
1	P–Pd	2.249 (1)	2.242 (1)
2	P–Pd–C(17)	82.4 (2)	82.2 (3)
3	P–Pd–N	176.5 (2)	175.9 (2)
4	C(24)–P–C(27)	113.0 (3)	106.2–111[b]

[a] The numbers used to identify the carbon atoms in the angles listed below correspond to the numbering scheme for **2f** in the paper. [b] The *tert*-butyl and isopropyl substituents in complex **2f** were disordered over two positions. The range between the largest and the shortest bond angles is shown.

complexes from these less hindered chloride precursors led to a complex mixture of products. However, less dramatic changes to the steric properties led to isolable species; the monomeric Pd-diarylamido complex **2f**, which is analogous to **2a** but containing a ligand derived from benzyl(*tert*-butyl)(isopropyl)phosphine, was synthesized in pure form by the same route used to prepare **2a**.

The structure of the 2-((*t*-Bu)(*i*-Pr))$PCH_2C_6H_4$-ligated complex **2f** was determined by X-ray crystallography (Figure 1), and this analysis showed that the hydrogen atom in the isopropyl group is directed toward the opposing *tert*-butyl group and that the isopropyl methyl groups face the coordination site occupied by the THF molecule. Thus, the steric effects imparted by the di-*tert*-butyl phosphino and *tert*-butyl(isopropyl)phosphino groups on the coordination site that would be occupied by the alkene ligand are not as large as one might first envision. Selected bond angles and lengths of the 2-(*t*-Bu)$_2PCH_2C_6H_4$-ligated **2a** and **2f** are listed in Table 1. The structures are similar to each other, but the C(24)–P–C(27) angle between the quaternary carbon atom of the *tert*-butyl group and the tertiary carbon of the isopropyl group in **2f** (109.2°) is about 3.8° smaller than the angle between the two quaternary carbons of the *tert*-butyl groups in **2a** (113.0°). The smaller size of the C–P–C angle in complex **2f** causes the alkyl substituents on the phosphorus atom of **2f** to be placed closer to the square plane than they are in complex **2a**.

While the steric environment around the palladium center of 2-((*t*-Bu)(*i*-Pr))$PCH_2C_6H_4$-ligated **2f** is not dramatically different from that of **2a**, this difference in steric property did affect the structure of the ground state. Significant amounts of the unsymmetrical dinuclear species **4f** (Scheme 2) were observed at room temperature by solution NMR spectroscopy, whereas the analogous dinuclear species **4a** containing di-*tert*-butylphosphino groups was observed in an equilibrium with the THF-free complex **3a** only at low temperatures.

Three-coordinate amido complexes that lack bound THF would form alkene adducts more readily than the THF-ligated species. To generate amido complexes lacking bound solvent, we conducted the synthesis of the amido complexes in the absence of THF or other basic solvents. The reaction of the cyclometalated palladium chloride dimers with excess $KNPh_2$ in toluene formed the solvent-free amido complexes **3a**, **3f**, **3g**, and **3h**. Longer reaction times were needed to prepare **3f**, **3g**, and **3h** than was needed to prepare cyclometalated benzyl phosphine amido complex **3a**. After one day, all of the chloride complexes **1f**, **1g**, and **1h** were consumed, but intermediates, presumed to be complexes containing bridging chloride and amido groups, were the primary products. After stirring an additional 1–6 days, these intermediates reacted with additional $KNPh_2$ to generate the desired products. Recrystallization of the crude material from reactions conducted at room temperature gave pure samples of the THF-free amido complexes in acceptable yields of 26–66%. Conducting these reactions at higher temperatures to increase the reaction rate led to the formation of two new, unknown species, as determined by ^{31}P NMR spectroscopy, and reactions at higher temperatures were not pursued further.

Reaction of Palladium-Diarylamido Complexes with Alkenes. The THF-ligated diarylamido complexes reacted with ethylene and α-olefins to generate enamine products (Scheme 3). Reactions of **2a**, **2f**, **2g**, and **2h** with ethylene in toluene-d_8 occurred at −10 °C to generate *N*-vinyldiphenylamine, Pd[P(*t*-Bu)(R)(Bn*)]$_2$ (R = *t*-Bu or *i*-Pr; Bn* = $-CH_2$-3-R′-C_6H_4,

dx.doi.org/10.1021/ja205722f |*J. Am. Chem. Soc.* 2011, 133, 15661–15673

R′ = H, CF_3, OCH_3) and Pd black. All reactions generated greater than 75% yield of *N*-vinyldiphenylamine. The enamine was characterized by comparison of the ^{1}H NMR spectrum to that of genuine material prepared independently. The Pd(0) complex Pd[P(*t*-Bu)(R)(Bn*)]$_2$ was the only species detected by ^{31}P NMR spectroscopy, and no palladium black was formed in the presence of 1 additional equivalent of P(*t*-Bu)$_2$(Bn).

The THF-free amido complexes **3a**, **3f**, **3g**, and **3h** also reacted with ethylene to generate *N*-vinyl diphenylamine and Pd[P(*t*-Bu)(R)(Bn*)]$_2$ in toluene-d_8. These reactions occurred below room temperature (−50 °C) to form enamine products in greater than 75% yield. Again, Pd[P(*t*-Bu)(R)(Bn*)]$_2$ was the only palladium product detected by ^{31}P NMR spectroscopy. The rates of the reactions of **3a**, **3f**, **3g**, and **3h** at −50 °C were similar to those of the THF-ligated species at the higher temperature of −10 °C.

Complex **2a** also reacted with vinylarenes in high yield, but this reaction occurred with regioselectivity distinct from the reactions of alkenes. The reaction of palladium-amide **2a** with 10 equiv of styrene in benzene-d_6 at 60 °C generated (*E*)-*N*-benzylidene-1,1-diphenylmethanamine in 78% yield (eq 1). In contrast to the reaction of 1-octene with **2a** that forms enamine products from 1,2-insertion into the metal−nitrogen bond, followed by *β*-hydrogen elimination (Figure 1),[43] the reaction of styrene formed only the enamine product from initial 2,1 insertion into the metal−nitrogen bond. Presumably, the formation of this isomer is favored by a combination of the steric interaction of the aryl group on the alkene with the two aryl substituents at nitrogen and the electronic preference for formation of an intermediate with the aryl group located α to the palladium center.[18] The identity of the organic products from reaction with substituted styrenes was confirmed by independent synthesis through palladium-catalyzed coupling of the corresponding *trans*-α-bromostyrene with $HNPh_2$. The regioselectivity of this process contrasts with that for reactions of [Rh(PEt$_3$)$_3$(NHAr)] and [Rh(PEt$_3$)$_3$(NAr$_2$)] with styrene, which formed ketimine and branched enamine products, respectively.[29]

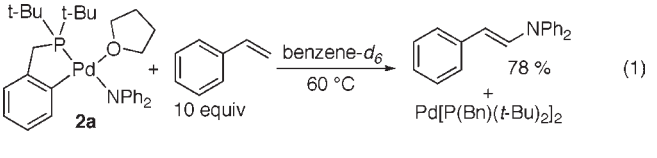

(1)

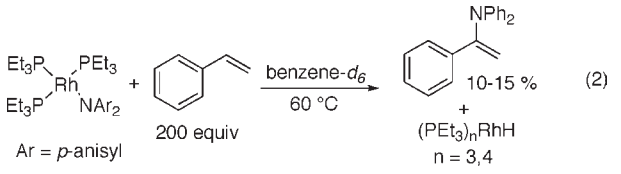

(2)

Palladium amido complex **2a** containing the cyclometalated benzylphosphine ligand is much more reactive toward alkene insertion than the isoelectronic [Rh(PEt$_3$)$_3$(N(*p*-anisyl)$_2$] complex.[29] This rhodium complex reacted with styrene to form only 10−15% of the enamine product in the presence of 200 equiv of styrene at 60 °C (eq 2), whereas the palladium complexes formed the enamine product at room temperature in good yield with less than 10 equiv of styrene.

Nonproductive Reactions of Amide 2a. To obtain high yields of the enamine from the reactions of alkenes and vinylarenes with amido complexes **2a**, **2f**−**2h**, **3a**, and **3f**−**3h**, the reactions must be conducted under strictly anhydrous conditions. Preparation of the amido complex in solvents that were not carefully dried generated palladium amido hydroxo complex **5** shown in Figure 2 (identified by NMR spectroscopy and X-ray diffraction; see the Supporting Information). Reactions of the amido complex with ethylene in the presence of adventitious water generated the same hydroxo amido complex.

Comparison of Ethylene and THF Binding to Palladium-Amide 3a. To measure the rate of migratory insertion directly, the equilibrium constants for dissociation of THF and binding of ethylene to the unsaturated species are needed to ensure that kinetic measurements are conducted under conditions in which the alkene-amido complex is the major species and the observed rate constant corresponds as close as possible to that for the migratory insertion step. The THF-bound amido complex **2a** equilibrates with the combination of free THF and the three-coordinate amido species **3a** on the NMR time scale (eq 3). This equilibration was revealed by the large difference in ^{31}P NMR chemical shifts of the THF-ligated amide **2a** in THF-d_8 (δ 88.0 ppm) and benzene-d_6 (δ 98.7 ppm). For reference, the ^{31}P NMR chemical shift of **3a** in benzene-d_6 was δ 101.7 ppm. The equilibrium constant for dissociation of THF from **2a** at 22 °C

Scheme 3. Reactions of THF Ligated Pd-Amides 2a, 2f−h, and THF-Free Palladium-Amides 3a, 3f−h, with Ethylene

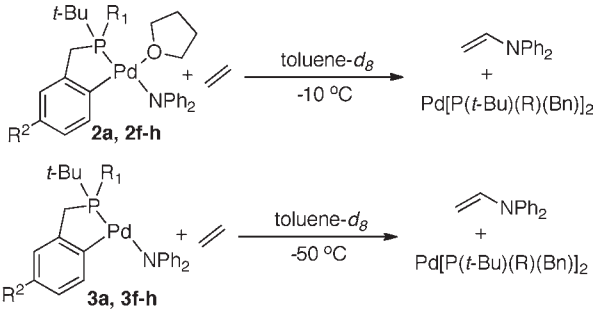

2a/3a R^1 = *t*-Bu, R^2 = H
2f/3f R^1 = *i*-Pr, R^2 = H
2g/3g R^1 = *t*-Bu, R^2 = CF_3
2h/3h R^1 = *t*-Bu, R^2 = OMe

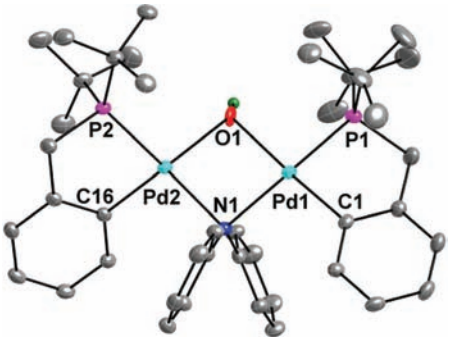

Figure 2. ORTEP drawing of **5** with 35% probability ellipsoids (the hydrogen atoms, except for the hydoxyl hydrogen, were omitted for clarity).

was determined more precisely by obtaining spectra of samples of **2a** containing different concentrations of THF in toluene-d_8. The equilibrium constant was determined to be 6.8 M^{-1} at room temperature from a fit of the plot (Figure 3) of the ^{31}P chemical shift vs the concentration of added THF to eq 4.

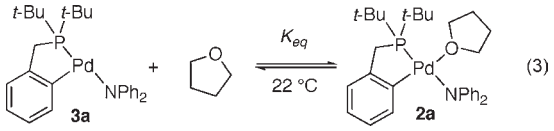

(3)

$$\delta_{obs} = \frac{\delta_{3a} + K_1\delta_{2a}[THF]}{1 + K_1[\mathbf{3a}][THF]} \quad (4)$$

The chemical shift of THF-bound **2a** also depended on temperature, due to the change in the equilibrium constant for dissociation of THF with temperature. The chemical shift at −60 °C was δ 88.0 ppm; the chemical shift at 40 °C (101.1 ppm) was closer to that of the THF-free species **3a**. From the observed chemical shifts at various temperatures, the equilibrium constants for the association of THF shown in eq 3 were determined (see Supporting Information), and from the temperature dependence of the equilibrium constants, the enthalpy and entropy were found to be ΔH = −11.3 kcal/mol and ΔS = −34.0 cal/mol. The enthalpy corresponds to the Pd−O bond strength.

We previously reported that the THF-free complex **3a** equilibrates with the ethylene-amido complex **8** in the presence of ethylene and determined that the equilibrium constant for ethylene binding at −65 °C is 0.09 (ΔG = 1.0 kcal/mol).[43] If we assume the entropy for binding of ethylene is similar to that for binding of THF, then the Pd−ethylene bond dissociation enthalpy is −6.1 kcal/mol, and the Pd−ethylene bond is weaker than the Pd−THF bond. These data are consistent with the lack of observation by ^{31}P NMR spectroscopy of an ethylene complex during the reaction of THF-ligated amido complex **2a** with 50 equiv of ethylene at −10 °C.

Mechanism of the Reaction of Ethylene with Palladium-Amide 2a. As previously reported, the addition of ethylene to the THF-free amido species **3a** at −65 °C generates a rapidly equilibrating mixture of **3a** and ethylene amido complex **8** (Scheme 4). In addition, the monomeric Pd-amido species **3a** partially converts to the unsymmetrical dimer **4a** in an equilibrium process at low temperature. The olefin-amido complex undergoes insertion at −50 °C. At −50 °C, two resonances corresponding to the dinuclear species are observed in the ^{31}P NMR spectrum, in addition to the resonance observed for **8**. These two complexes decay in concert, implying that the equilibrium between **3a** and **4a** is established faster than the olefin insertion process.

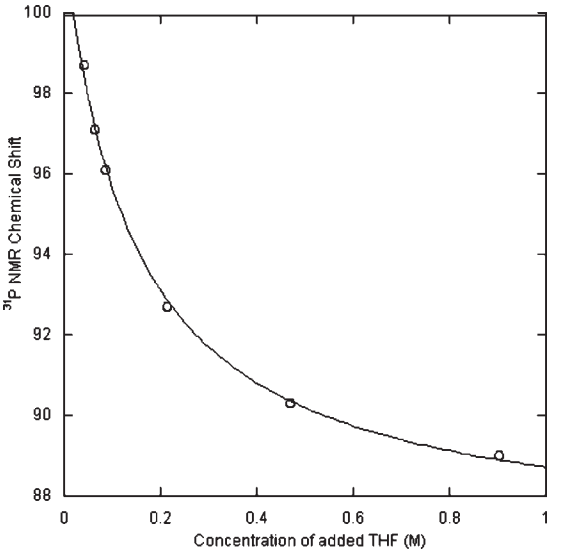

Figure 3. Plot of ^{31}P chemical shift of **3a** versus concentration of added THF. The data were fit to eq 4.

The equilibria involving binding of THF and ethylene to amido complex **3a** described in this paper, along with the previously reported data concerning the reaction of ethylene amido species **8**, support the mechanism shown in Scheme 4 for the reaction of palladium-diarylamides **2a** and **3a** with ethylene. In this mechanism, THF rapidly and reversibly dissociates from complex **2a**, and the resulting THF-free complex **3a** binds ethylene to generate the olefin-amido adduct **8**.[44] Complex **8** then undergoes migratory insertion to generate the proposed alkylpalladium intermediate **9**. Intermediate **9** then rapidly decomposes by β-hydrogen elimination to form a Pd-hydride complex (**10**), and complex **10** undergoes C−H bond-forming reductive elimination to generate Pd[P(Bn)(*t*-Bu)$_2$]$_2$ (**11**) and Pd black. In the presence of excess P(Bn)(*t*-Bu)$_2$, the unsaturated product of reductive elimination binds the phosphine, and

Scheme 4. Proposed Reaction Mechanism of the Reaction of Pd-Amides 2a and 3a with Ethylene

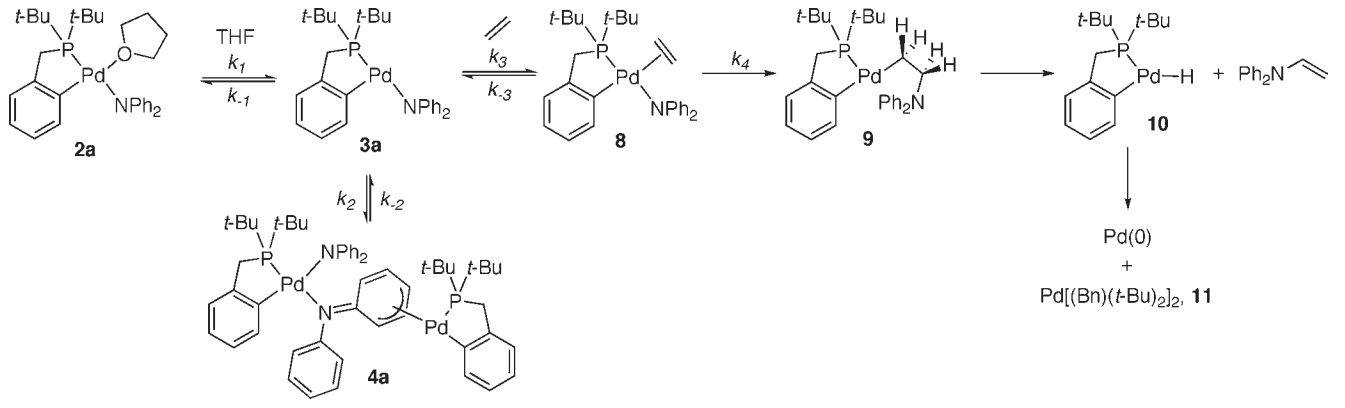

dx.doi.org/10.1021/ja205722f |*J. Am. Chem. Soc.* 2011, 133, 15661–15673

Scheme 5. Simulated Reaction Mechanism of Pd-Amide 3a with Ethylene

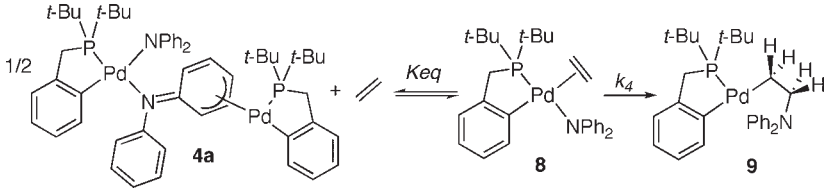

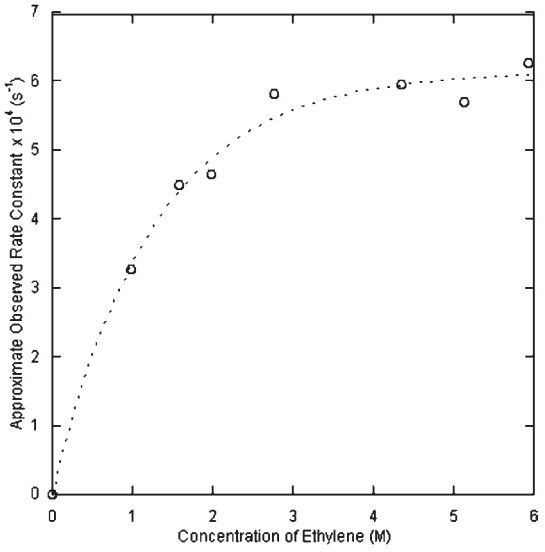

Figure 4. Approximate observed rate constant[45] for the reaction of **3a** with ethylene vs the concentration of added ethylene. For a comment on the approximation of the rate constants, see footnote.[45]

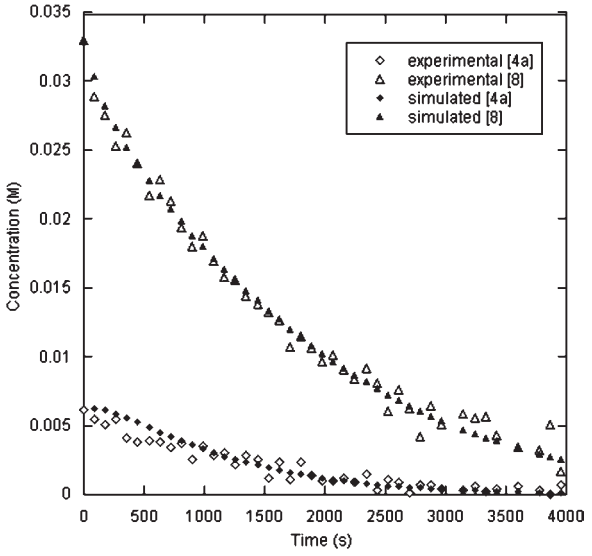

Figure 5. Experimental and simulated decay curves of the reaction of **3a** with ethylene.

$Pd[P(Bn)(t\text{-}Bu)_2]_2$ is the only product observed by ^{31}P NMR spectroscopy. Intermediates **9** and **10** were not observed during the course of the reaction.

Reactions of Alkene-Amido Complex 8. To gain information on the rate constant of the individual insertion step (k_4), the observed rate constant for the reaction of the pure olefin-amido complex **8** was measured at different concentrations of ethylene. If the mechanism in Scheme 4 is followed, then the value of k_{obs} should approach the value of the insertion step under conditions in which the equilibrium lies far toward the ethylene amido complex **8**. A plot of the approximate k_{obs}[45] for the reaction of **3a** vs the concentration of ethylene is shown in Figure 4. At low concentrations of ethylene, the rate is positively dependent on the concentration of ethylene, but at high concentrations, the rate constant approaches a constant value.

Under conditions in which **3a** is allowed to react with high concentrations of ethylene (150 equiv), the concentration of the olefin adduct is much larger than the concentration of the three-coordinate monomer **3a**, and the kinetic expression corresponding to the mechanism in Scheme 4 can be simplified. However, fitting of the dependence of k_{obs} on [ethylene] is complicated by the equilibrium between **3a** and the unsymmetrical dimer **4a**. Fortunately, the olefin adduct **8** equilibrates with the unsymmetrical dimer **4a** and free ethylene faster than it undergoes migratory insertion. During the reaction of **3a** with 150 equiv of ethylene, 15% of the unsymmetrical dimer **4a** was observed by ^{31}P NMR spectroscopy, and the resonances for **4a** decay in concert with that observed for the ethylene adduct **8**.

To determine precisely the rate constant for the migratory insertion step (k_4), we simulated the kinetic data of the simplified process in Scheme 5 with the software *KINSIM*[46] and iteratively fit the experimental decays of **4a** and **8** over time to the simulated data with the software *FITSIM*.[47] The experimental data fit the simulated decay curves well (see Figure 5), and this analysis showed the rate constant for the C−N bond-forming migratory insertion step (k_4) to be $(8.7 \pm 0.5) \times 10^{-4}$ s^{-1}.

Steric Effects of the Ancillary Ligand. To evaluate the steric effects of the ancillary ligand on the migratory insertion step, we compared the structure and reactivity of amido complex **2f** ligated with a cyclometalated (*tert*-butyl)(isopropyl)benzylphosphine ligand to those of the complex **2a** ligated by the cyclometalated di(*tert*-butyl)benzylphosphine ligand. The rate constants for the reactions of THF-ligated complexes **2a** and **2f** with ethylene are shown in eq 5. These observed rate constants correspond to the product of the equilibrium constant for the exchange of ethylene for THF and the rate constant for the migratory insertion step. The reaction of the less hindered **2f** was faster than that of **2a**, but by approximately the sum of the standard deviations. The similarity in the rate constant for reaction of **2a** and **2f** could be due to similar equilibrium constants for binding and insertion of ethylene by the two complexes or to counterbalancing steric effects on the binding

dx.doi.org/10.1021/ja205722f |*J. Am. Chem. Soc.* 2011, 133, 15661–15673

and insertion step. The following experiments and computations distinguish between these possibilities.

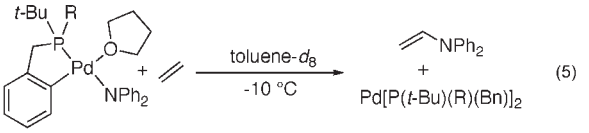

2a, R = *t*-Bu $k_{obs} = 4.6 \pm 0.3 \times 10^{-4}\ s^{-1}$
2f, R = *i*-Pr $k_{obs} = 5.3 \pm 0.5 \times 10^{-4}\ s^{-1}$

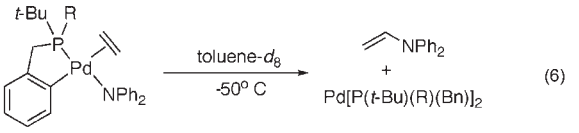

3a - ethylene adduct (**8**), R = *t*-Bu $k_{mig\ ins} = 8.7 \times 10^{-4}\ s^{-1}$ ($\Delta G^{\ddagger}$ = 16.0 kcal/mol)
3f - ethylene adduct, R = *i*-Pr $k_{mig\ ins} = 0.97 \times 10^{-4}\ s^{-1}$ ($\Delta G^{\ddagger}$ = 17.0 kcal/mol)

The rate constants for migratory insertion of ethylene into the Pd−N bond of complexes **3a** and **3f** are shown in eq 6. In contrast to the reactions of **3a**, the reaction of the 2-((*t*-Bu)-(*i*-Pr))$PCH_2C_6H_4$-ligated **3f** with ethylene at −50 °C did not contain measurable quantities of the unsymmetrical dimer **4f** after the pre-equilibrium for binding of ethylene had been established. After addition of ethylene, the amount of the ethylene adduct was small, but after approximately 20 min (vs a $t_{1/2}$ = 2 h for the insertion process), the dinuclear species **4f** was completely converted to the ethylene adduct of **3f**. Thus, the decay of this adduct was measured after the pre-equilibrium had been established, and this portion of the data were fitted to an exponential decay to determine the rate constant for migratory insertion. The rate constant for insertion of ethylene into the less sterically encumbered amido complex **3f** was $0.97 \times 10^{-4}\ s^{-1}$ ($\Delta G^{\ddagger}$ = 17.0 kcal/mol). This rate constant is almost an order of magnitude smaller than the rate constant for insertion of ethylene into the more sterically encumbered complex **3a** ($8.7 \times 10^{-4}\ s^{-1}$, ΔG = 16.0 kcal/mol). These results suggest that steric hindrance at the phosphorus atom decreases the barrier to the C−N bond-forming step of the migratory insertion process.

Computed Free Energy Barriers for Insertion of Ethylene into the Pd−N Bonds of Amido Complexes 3a and 3f. To evaluate further the effect of the steric environment around the palladium atom on the migratory insertion process, a series of computations were performed on the reaction of olefin amido complexes **3a** and **3f**. These computations were conducted using density functional theory as implemented by the *Gaussian 09* package.[48] The B3LYP functional with polarized triple-ζ basis sets has been shown to generate accurate results for many palladium systems[49−51] and was, therefore, used for calculations of the reactivity of **3a**, **3f**, and an analogous complex ligated by a truncated 2-$(CH_3)_2PCH_2C_6H_4$ ligand.

Because the precise structure of the ethylene amido complex **8** is unknown, reactions of the two isomers of **8** with the alkene *cis* or *trans* to the phosphorus atom were computed. The *cis* isomer contains the alkene in the coordination site of the THF in complex **2a.** The ground state of the *cis* isomer is lower than that of the *trans* isomer by 2.4 kcal/mol, and the free energy of activation from the *cis* ground state to the *cis* transition state was 0.5 kcal/mol lower than the free energy of activation from the *trans* ground state to the *trans* transition state. Thus, to determine the steric effect of the ancillary ligand on the migratory insertion step,

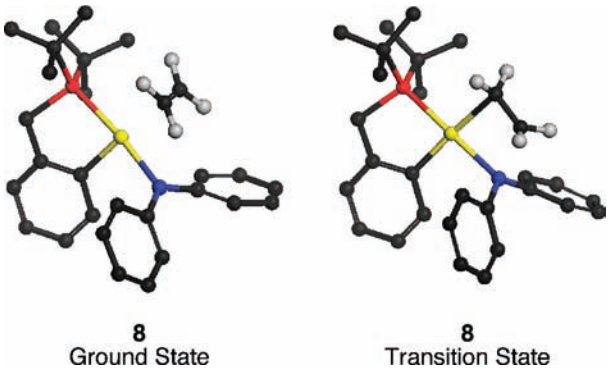

Figure 6. Optimized ground state and transition state structure of the olefin amido adduct **8**.

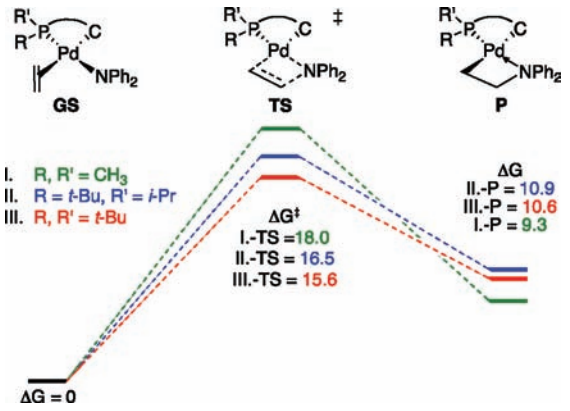

Figure 7. Optimized ground state and transition state free energies for ethylene insertion into P−C ligated Pd-amido complexes.

the reactions of ethylene with the *cis* isomers of a series of olefin amido complexes ligated by 2-((*t*-Bu)(*i*-Pr))$PCH_2C_6H_4$ and 2-$(CH_3)_2PCH_2C_6H_4$ were computed.

The optimized ground-state structure of **8**, and the structure of the transition state for the insertion reaction of **8** are shown in Figure 6. In the ground-state structure of **8**, the centroid of the ethylene ligand lies in the square plane, and the C−C double bond is oriented perpendicular to that of the square plane. The computed distance of the Pd-ethylene bond is 2.50 Å. In the transition state structure for insertion, the olefin has rotated approximately 90° and lies parallel to the Pd−N bond. The distance between the palladium and the closest ethylene carbon is 2.27 Å, and the C−N distance is 2.04 Å. The hydrogen atoms on the ethylene are splayed away from the Pd-center, and the H−C−H angle is 106°, which is less than the 109° of an sp^3 hybridized carbon.

The immediate product from the insertion process has an azametallocyclobutane structure in which the nitrogen atom forms a dative bond to the palladium center. The angles at the β-carbon of this product indicate that the ethylene carbons are hybridized in an sp^3 fashion. The Pd−C distance (2.14 Å) is typical for a palladium−carbon bond, and the C−N distance (1.52 Å) is typical for a C−N single bond.

The computed free energies for migratory insertion of ethylene into the amido complexes containing the three cyclometalated ligands, 2-$(t\text{-Bu})_2PCH_2C_6H_4$, 2-((*t*-Bu)(*i*-Pr))$PCH_2C_6H_4$, and 2-$(CH_3)_2PCH_2C_6H_4$, are shown in Figure 7. The free energy of activation for reaction of complex **8**, which is ligated

by the bulkiest ligand 2-(t-Bu)$_2$PCH$_2$C$_6$H$_4$ was computed to be the lowest (15.6 kcal/mol). The enthalpy of activation of this process (14.0 kcal/mol) was computed to be close to that of the free energy, indicating that the entropy for this process has the small value expected for an intramolecular reaction. The free energy barrier for reaction of the 2-((*t*-Bu)(*i*-Pr))PCH$_2$C$_6$H$_4$-ligated complex was computed to be about 1 kcal/mol higher (16.5 kcal/mol) than that of the 2-(t-Bu)$_2$PCH$_2$C$_6$H$_4$-ligated complex, and the free energy barrier for reaction of the least bulky complex ligated by 2-(CH$_3$)$_2$PCH$_2$C$_6$H$_4$ to be the highest (18.0 kcal/mol). These computed free energies are consistent with the activation barriers measured experimentally. The difference in free energies determined experimentally for reaction of **3a** and **3f** was 1.0 kcal/mol. Thus, both the experimental and computational results indicate that greater steric bulk on the phosphorus atom leads to a lower barrier for migratory insertion, even though the coordination number of the complex does not change during insertion of an alkene into an amido complex.

An analysis of the computed structures of the ground and transition states provides a rationalization for the steric effect. In the computed ground-state structure, the olefin is located *cis* to the phosphorus atom, and the steric interactions between the ethylene hydrogens and the alkyl groups on the phosphorus atom are greater than they would be in other conformations. As the complex adopts the structure of the transition state in which the C−C bond lies parallel to the Pd−N bond, the distances between the alkyl groups on the phosphorus atom and the termini of the alkene ligand decrease. This decrease in steric interaction from the ground to transition state is consistent with the lower barrier for reaction of the more hindered complex.

Although the barrier for the migratory insertion step for the more sterically congested complex is lower than that for the less sterically congested complex, the reactions of ethylene with the THF-ligated amides **2a** and **2f** are not faster for the more hindered complex than for the less hindered compound. The difference between the rates of reaction of the sterically more and less hindered complexes containing and lacking bound THF results from a difference in binding energy of ethylene and THF to the more and less hindered amidopalladium fragments. Details on the measurement of these equilibrium constants for **3f** are provided in the Supporting Information and the determination of this value for the binding of ethylene to **3a** was included in reference 43. The K_{eq} at 22 °C for binding of THF to the less sterically congested **3f** is 14 M^{-1}, whereas the K_{eq} for binding of THF to the more hindered **3a** is 6.8 M^{-1} (ratio of K_{eq} values = 2). The K_{eq} at −65 °C for binding of ethylene to **3f** is 149 M^{-1}, whereas the K_{eq} for binding of ethylene to **3a** is 11 M^{-1} (ratio of K_{eq} values = 13). These data demonstrate that the binding affinity of THF to the less sterically congested **3f** is two times greater than the binding affinity of THF to **3a**. However, the binding affinity of ethylene to **3f** is about 13 times greater than the binding affinity of ethylene to **3a**. Although the ethylene adduct of the THF-free amido complex **3f** has a 1.0 kcal/mol higher barrier for the migratory insertion step than the ethylene adduct of **3a**, the difference in binding of ethylene to **3f** and **3a** is larger than that for binding of THF, and this difference leads to the slightly faster overall rate for the reaction of **2f** with ethylene than for the reaction of **2a** with ethylene.

Steric effects on migratory insertion reactions have rarely been evaluated.[52,53] The binding equilibrium and the migratory insertion step are rarely separated, and the direct precursor to insertion is rarely observed directly.[54−58] In one case, Bercaw did report insertions of propene into the niobium−hydride and tantalum−hydride bonds of metal alkene hydride complexes.[53] The rate constants measured for insertion of permethylmetallocene and unsubstituted metallocene propylene hydride complexes followed the trend Cp*$_2$Nb(CH$_2$=CHCH$_3$)H > Cp$_2$Nb(CH$_2$=CHCH$_3$)H > Cp*$_2$Ta(CH$_2$=CHCH$_3$)H > Cp$_2$Ta(CH$_2$=CHCH$_3$)H. The authors attributed this trend to the greater steric interactions between the methyl group of the propene and the methyl groups on the Cp* ligands in the ground states than in the transition states. In the ground state, the olefin lies in the plane bisecting the two Cp* ligands and the hydrogen atoms and methyl group on the alkene are pointed toward the methyl groups on the Cp* ligand. The transition state structure is less sterically congested because the methyl group becomes more distant from the Cp rings as the product alkyl ligand emerges. This change in structure and accompanying decrease in steric effects from the ground to transition state leads to the faster rate for insertion of the permethylmetallocene derivatives.

Electronic Effects of the Ancillary Ligand. To examine the electronic effect of the ancillary ligand on the rate of migratory insertion, THF-ligated, palladium-diarylamido complexes were synthesized that contain substituents in the 3-position of the benzylphosphine aryl ring. Complex **2h**, which contains an electron-withdrawing trifluoromethyl group and complex **2g**, which contains an electron-donating methoxy group in this position on the benzylic aryl ring, were allowed to react with ethylene in toluene at −10 °C. The decay of the palladium-amide was monitored by ^{1}H NMR spectroscopy, and the rate constants for reactions of these complexes and the unsubstituted complex **2a** are shown in eq 7. Trifluoromethyl-substituted **2h** reacted about 2.5 times faster than the parent complex **2a**, and complex **2a** reacted slightly faster than methoxy-substituted **2g**.

These observed rate constants are a composite of the equilibrium constants for exchange of ethylene for THF and the rate constant for insertion. Thus, to measure the electronic effects of the ancillary ligand on the individual migratory insertion step, the reactions of ethylene with the benzylphosphine-ligated amido complexes **3a**, **3g**, and **3h** lacking a THF were conducted. Complexes **3a**, **3g**, and **3h**, were allowed to react with a large excess of ethylene at −50 °C, and the decay was monitored by ^{31}P NMR spectroscopy. The rate constants for the migratory insertion step with complexes **3a** and **3g** were determined by kinetic simulation as described earlier in this paper. Because the reaction of **3h** with ethylene did not form an observable amount of dimer **4h**, the rate constant for migratory insertion could be determined directly from the exponential decay of the ethylene adduct of **3h**. The reaction rates and the free energies of activation are listed in eq 8. The trifluoromethyl-substituted complex **3h** reacted about two times faster than the unsubstituted complex **3a**, and complex **3a** reacted about two times faster than the methoxy-substituted complex **3g**. These kinetic data indicate that the complexes in this series containing a more electron-poor metal center undergo the elementary migratory insertion step faster than those containing a more electron-rich metal center.

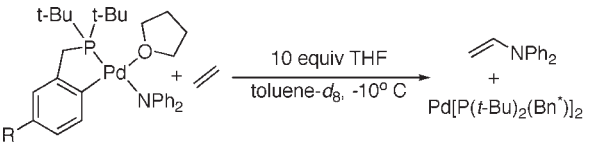

(7)

2h, R = CF$_3$ k_{obs} = 1.0 ± 0.04 x 10^{-3} s^{-1}
2a, R = H k_{obs} = 4.6 ± 0.3 x 10^{-4} s^{-1}
2g, R = OCH$_3$ k_{obs} = 3.9 ± 0.2 x 10^{-4} s^{-1}

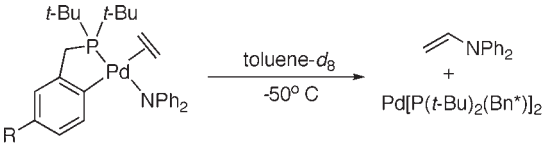

(8)

3h - ethylene adduct, R = CF_3 $k_{mig\ ins} = 2.6 \pm 0.2 \times 10^{-3}\ s^{-1}$
3a - ethylene adduct (**8**), R = H $k_{mig\ ins} = 8.7 \times 10^{-4}\ s^{-1}$
3g - ethylene adduct, R = OCH_3 $k_{mig\ ins} = 3.8 \times 10^{-4}\ s^{-1}$

The trend observed for the insertions of ethylene into the metal−nitrogen bond of palladium-amido complexes parallels the trends observed for insertion of ethylene into metal−carbon and metal−hydrogen bonds. Generally, complexes containing more electrophilic metal centers undergo migratory insertion faster than those containing less electrophilic centers.[59,60] However, it is difficult to deduce whether the equilibrium constant for binding of the olefin or the rate constant for migratory insertion is responsible for the faster rates typically observed for the insertions of more electron-poor metal centers, because increasing the electrophilicity of the metal center typically results in stronger binding of the olefin.

A comparison of the rates of migratory insertion of the palladium−amido complexes and more electrophilic lanthanide and group IV amido complexes can be made, although one must appreciate that there are multiple differences between the structures and the reactions of the early metal systems and the palladium complexes. The amido groups in the more electrophilic amido complexes (alkylamides) are different from those in the palladium amido complexes reported here (diarylamides), and the reactions of the lanthanide systems are intramolecular, whereas the reactions of the palladium amides are intermolecular. Despite these differences, the two types of complexes undergo insertion of alkenes into metal-amido linkages with similar rates.

Marks and co-workers reported computational and experimental studies of the mechanism of the cyclization of aminoalkenes catalyzed by organolanthanide complexes containing permethylcyclopentyldienyl ligands.[25,61] This work showed that the free energy of activation ($\Delta G^{\ddagger}$) for the migratory insertion of an alkene unit within a cyclic lanthanide aminoalkene complex is roughly 21−24 kcal/mol.[62] Thus, this free energy of activation for insertion of an alkene into a more electrophilic lanthanide-amido complex is higher than the 16 kcal/mol free energy barrier for insertion of ethylene within the amidopalladium olefin complex **8**. However, the entropic contribution to the $\Delta G^{\ddagger}$ for insertion into the lanthanide amides was found to be large. The computed $\Delta H^{\ddagger}$ for the migratory insertion of ethylene within complex **8** of 14.0 kcal/mol is similar to the experimentally measured $\Delta H^{\ddagger}$ barrier of 12.7 kcal/mol for organolanthanide complexes. Of these two values, $\Delta H^{\ddagger}$ would be most affected by the electronic properties of the two systems. Perhaps the effect of the greater electrophilicity of the lanthanide amide complexes and the greater bond strength of the lanthanide amides counterbalance each other.

The free energy barriers for insertions of alkenes into group IV amides are also higher than those for the palladium amides. The hydroamination of an aminoalkene catalyzed by constrained-geometry *ansa*-ligated Zr complexes occurred over days at 100−120 °C.[22,63] This reaction was proposed to occur by turnover-limiting insertion of the alkene into the metal−amido bond. The elevated temperatures and long times required for cyclization indicate that the barrier for insertion of the alkene into the Zr−N bond is much higher than that for insertion into both the lanthanide−amide and palladium−amide bonds. This higher barrier for reaction of the ziroconium complex likely results from an increased strength of the metal−nitrogen bond due to π-donation of the amide lone pair to the d^0 metal center.[64,65] This comparison of the barriers to group IV amides is made tentatively because the entropy and enthalpy of activation for insertions into the group IV amido complexes have not been reported.

Table 2. Reactivity of Palladium-Amide 2a with Functionalized

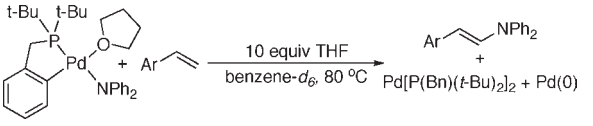

Entry	Styrene	Product	Yield (%)	k_{obs} (s^{-1})
1	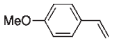	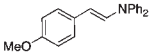	11	-
2		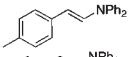	40	0.94×10^{-3}
3		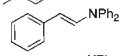	78	1.5×10^{-3}
4		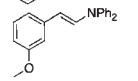	61	1.7×10^{-3}
5		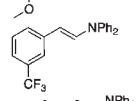	87	4.3×10^{-3}
6	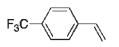	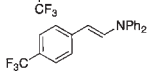	95	4.9×10^{-3}

Electronic Effects of the Olefin on the Rate of Insertion. The reactions of **2a** with a series of vinylarenes was conducted to reveal the effect of the electronic properties of the vinylarene on the rates of insertion. Amido complex **2a** was allowed to react with a series of vinylarenes containing electron-donating and electron-withdrawing substituents at the *meta* and *para*-positions, and the rate constants for these reactions were measured by ^{1}H NMR spectroscopy. The yields and rate constants for these reactions are summarized in Table 2.

In general, reactions of Pd-amide **2a** with electron-poor vinylarenes generated enamine products in higher yields than reactions of **2a** with electron-rich vinylarenes. The reaction of **2a** with *p*-(trifluoromethyl)styrene gave 95% yield of the (*E*)-β-aminoethylarene, whereas the reaction of amide **2a** with *p*-methoxystyrene gave only 11% yield of the enamine product. In the latter case, decomposition of the amido complex by protonation of the palladium−nitrogen bond was faster than migratory insertion.

Consistent with the difference in reaction yields, the reactions of complex **2a** with vinylarenes containing electron-withdrawing substituents were faster than those containing electron-donating substituents. For example, the reaction of **2a** with *p*-(trifluoromethyl)-styrene was more than three times faster than the reaction of **2a** with styrene. Likewise, the reaction of **2a** with styrene was almost two times faster than the reaction of **2a** with the more electron-rich *p*-methylstyrene. Figure 8 shows a Hammett plot of $\log(k_x/k_h)$ versus σ derived from the data in Table 2. The ρ value is 1.04 (r = 0.988). This positive ρ value indicates an accumulation of negative charge or a decrease in the partial positive charge on the olefin in the transition state for migratory insertion.

dx.doi.org/10.1021/ja205722f |*J. Am. Chem. Soc.* 2011, 133, 15661–15673

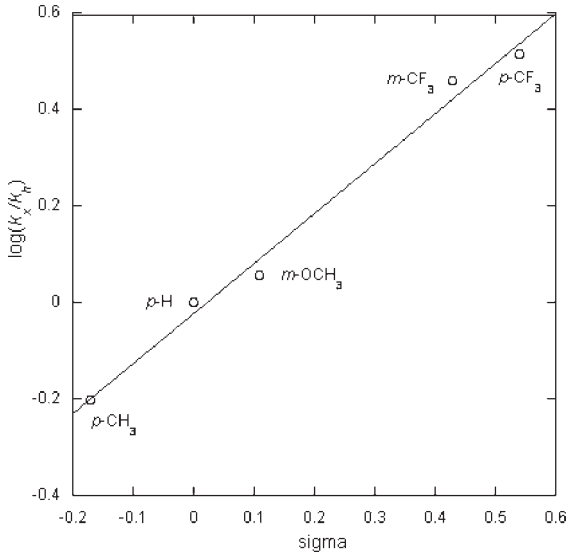

Figure 8. Hammett plot of the reaction of palladium-amide **2a** with substituted styrenes.

To begin to determine the origin of the observed electronic effects, we evaluated the relative binding affinities of the different vinylarenes. We attempted to generate the amido styrene complex from the reaction of amido complex **3a** lacking THF with styrene in benzene-d_8, but no change in the ^{31}P or ^{1}H NMR signals of complex **2a** was observed.[66] Thus, we assessed the relative binding energies of the vinylarenes to the benzylphosphine-ligated palladium-amido fragments using density functional theory. Although the differences in binding energies of the different vinylarenes are not large, the ground-state energies should be reliable, and the relative, rather than absolute, binding energies are the important values for this analysis.

The energies of the vinylarene-amido complexes containing 4-methylstyrene and 3-methoxystyrene were calculated. The initial structures were generated by replacing ethylene in the computed structures of the ethylene amido complex **8** with a vinylarene. The energies of four isomers with different orientations of the vinylarenes were minimized, and the same isomer was found to have the lowest energy for both vinylarenes complexes. The palladium−styrene bond is relatively long for a Pd−alkene bond (2.72 Å). The alkene unit is oreinted perpendicular to the square plane, and the aryl group of the styrene is located *cis* the phosphorus atom.

The computed relative free energies ($\Delta G°$) of the styrene-amido complexes are shown in the free energy diagram for reaction of THF-complex **2a** with 4-methylsytrene and 3-methoxystyrene (Figure 9). The complex of the more electron-rich vinylarene, 4-methylsytrene, was computed to be 1.2 kcal/mol more stable than the complex of 3-methoxystyrene, whereas the experimental free energy barrier ($\Delta G^{‡}$) for reaction of the 3-methoxystyrene complex was found to be 0.4 kcal/mol lower than that of 4-methylstyrene. As depicted in Figure 9, this combination of experimental and computational data imply that the free energy barrier for the elementary migratory insertion step of the 3-methoxystyrene complex is 1.6 kcal/mol smaller than that for the same reaction of the 4-methylstyrene complex.

Becuase electron-rich vinylarenes bind more strongly to the palladium center than electron-poor vinylarenes, the coordination of alkenes to this Pd(II) center involves a net flow of

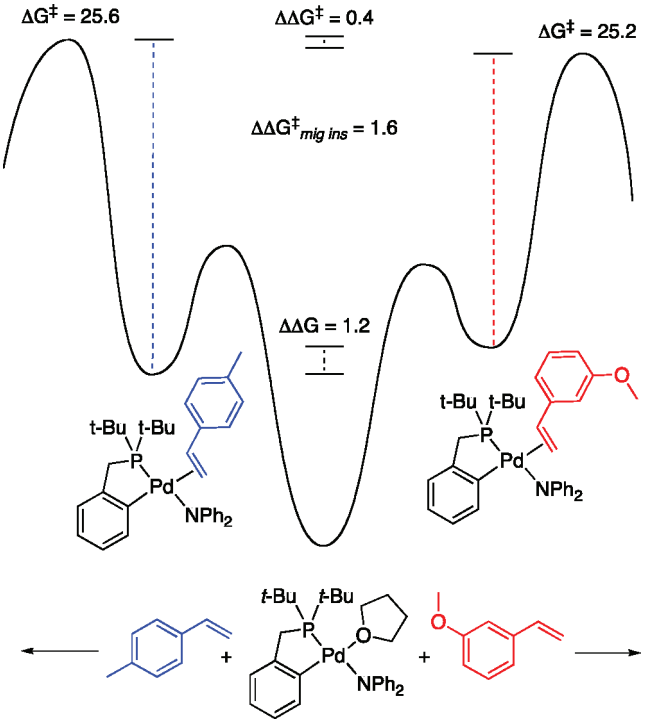

Figure 9. Energy diagram for the reaction of palladium-amide **2a** with substituted styrenes. The relative energies of the DFT-optimized, ground-state styrene complexes are shown. All energies have the units of kcal/mol.

Scheme 6. Reaction of Palladium-Amide 2a with Substituted Vinylarenes

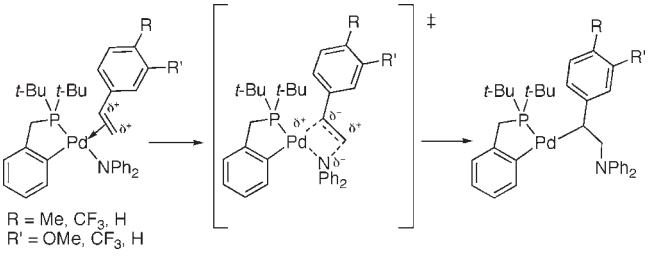

electrons from the alkene to the metal. Typically, the alkene in palladium-olefin complexes acts primarily as a σ donor.[67,68] The immediate product from insertion of the olefin into the metal−nitrogen bond is an aryl-substituted 2-aminoalkyl ligand that places a negative charge on the Pd-bound carbon. Therefore, we propose that the observed electronic effect results from a positively charged alkene ligand becoming a negatively charged alkyl ligand through a transition state that reflects this overall change in the property of the α-carbon of the vinylarene (Scheme 6).

Comparison of the Electronic Effects of the Alkene to Those of Insertions of Alkenes into Metal−Hydride and Metal−Alkyl Bonds. The ρ value observed for the insertion of substituted styrenes into the palladium−nitrogen bonds of palladium-amides (ρ = 1.04, r = 0.988) was similar to the ρ value obtained by Brookhart and co-workers (ρ = 1.1 ± 0.1, r = 0.991) during a study of the electronic effects of the migratory insertion of *para*-substituted vinylarenes into methylpalladium

dx.doi.org/10.1021/ja205722f |*J. Am. Chem. Soc.* 2011, 133, 15661–15673

Scheme 7. Reaction of *para*-Substituted Styrenes with Methyl Palladium Complexes

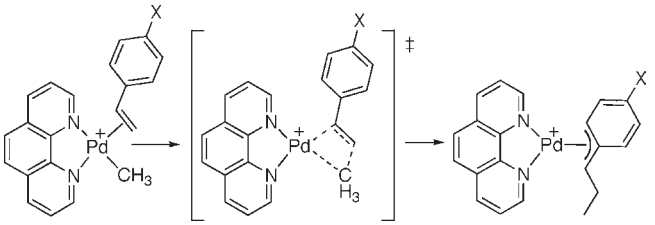

complexes (Scheme 7).[69] In this study, the binding affinities of the *para*-substituted styrenes were measured, and the relative free energies of activation ($\Delta\Delta G^{\ddagger}$) were determined. These data indicate that the effect of the electronic properties of the olefin on the relative energies of the ground states was larger than the effect of the electronic properties of the olefin on the relative energies of the transition states. This result parallels the trend we deduced from our studies of the rates of migratory insertion of substituted vinylarenes into Pd−N bonds.

The electronic effects on the coordination and insertion steps of the reaction of substituted vinylarenes with $RhH_2Cl(PPh_3)_3$ measured during early studies by Halpern were different from those deduced for the insertions into palladium amide and alkyl bonds.[70] Electron-poor styrenes bind to these rhodium complexes more strongly than do electron-rich styrenes, and the insertion of the styrene into the Rh−H bond was slower for electron-poor styrenes than for electron-rich styrenes. Similarly, Bercaw studied the binding of vinylarenes to a cyclopentadienyl-ligated niobium hydride complex and the subsequent migratory insertion of the styrene into the Nb−H bond. The ρ values for binding of the styrene to the Nb center and for the insertion reaction of *endo*-$Cp_2NbH(4\text{-}X\text{-}C_6H_4CH{=}CH_2)$ were +2.2, and −1.06, respectively.[53,71] These results demonstate that the more electron-poor, *p*-substituted vinylarenes form more stable adducts to these niobium complexes, (most likely due to increased π-backbonding from the metal to the alkene unit of the more electron-poor vinyalrene), but the complex of the more electron-poor vinylarene underwent the migratory insertion step more slowly than did the complex of the more electron-rich vinylarene.[53] Thus, the electronic effects observed for the migratory insertion of vinylarenes into the palladium-amides in the current work are the opposite of those observed for the insertions of vinylarenes into the metal−hydride bonds of hydridometal vinylarene complexes of niobium(III) and rhodium(III). Instead, they parallel the electronic effects on the insertions of vinylarenes into the palladium−carbon bonds of cationic Pd(II) vinylarene complexes.

■ SUMMARY

In this paper, we have reported studies on the migratory insertions of unactivated olefins into the Pd−N bond of isolated palladium-diarylamido complexes that reveal the steric and electronic effects of the ancillary ligand and olefin on the rate of the migratory insertion. By varying the electronic and steric properties of the ancillary benzylphosphine ligand, we revealed the effects of the structure of the ancillary ligand on the individual steps of alkene binding and insertion into the Pd−N bond. In addition, by conducting the reactions with a series of vinylarenes and computing the relative binding energies of the vinylarenes, we also revealed the effect of the olefin electronics on the individual steps of olefin binding and insertion. Understanding these effects on this new class of organometallic transformation is necessary for the rational design of new catalysts for the amination of olefins. The following conclusions have been drawn from these studies.

Steric Effects On the Insertion Process

(1) Bulky substituents on the phosphine create stronger steric interactions in the ground state than in the transition state for migratory insertion into the palladium amides. In the transition state, the alkene lies along the Pd−N bond, and the steric interactions between the alkene hydrogens and the alkyl groups on the phosphorus atom in the ancillary ligand are weaker than they are in the ground state. Because the steric interactions are greater in the ground state than in the transition state, the barrier for migratory insertion is lower for the complexes ligated with the bulkier phosphine than for the complex ligated by the smaller phosphine, as deduced by both experimental and computational work.

(2) The effect of the phosphine steric properties on binding of the alkene prior to the migratory insertion counterbalances the effect of these steric properties on the C−N bond-forming step, and this combination of effects causes the reactions initiated by the THF-ligated species with larger and smaller ligands to be similar to each other. Thus, careful balancing of the size of the ancillary ligand is needed to increase the rate of reaction of amido complexes with alkenes.

(3) The complex containing the more hindered ancillary ligand adopts more of the monomeric structure than the complex containing the less hindred ancillary ligand. Because insertion involves binding of the olefin *cis* to a terminal amide and the dimeric strutures form stable, unreactive amido species, monomeric amides are necessary for facile formation of the olefin-amido adduct.

Electronic Effects on the Insertion Process

(1) The amido complexes in this study containing the more weakly donating ancillary ligands, and therefore the more electrophilic metal centers, inserted alkenes faster than those containing the more strongly donating ancillary ligands. This result parallels the general trend in prior studies showing that alkene insertions into metal−alkyl bonds of complexes containing more electrophilic metal centers are faster than those into into metal−alkyl bonds of complexes containing more electron-rich metal centers.

(2) The rates of insertions of alkenes into the palladium-amides in this study are similar to those for insertions into the much more electrophilic lanthanide and Group IV amido alkene complexes. The similarity of these rates suggests that insertions of alkenes into metal−amide bonds could be as broad in scope as insertions of alkenes into metal−carbon bonds.

(3) The THF-ligated benzylphosphine-ligated palladium-amides reacted with electron-poor vinylarenes slightly faster than with electron-rich vinylarenes. The relative ground-state energies of styrene-bound amidopalladium complexes were assessed by DFT methods, and the complex of the more electron-donatining 4-methylstyrene

was computed to be more stable than the complex of the less electron-donating 3-methoxystyrene. This combination of the experimentally measured free energies of activation for the reaction of THF-ligated palladium amide with the different vinylarenes and the computed relative ground-state energies of the vinylarene complexes show that the elementary step of migratory insertion is faster for complexes of electron-poor vinylarenes than for complexes of electron-rich vinylarenes and that the difference in free energies of activation for this step is larger than that for the overall reaction initiated with the THF-ligated palladium amide.

Thus, we have provided in this article the first detailed account of the effect of the steric and electronic properties of the alkene and ancillary ligand on the rate and scope of the insertion of alkenes into palladium−nitrogen bonds. These complexes are the only metal-amido complexes that form directly observable olefin adducts. Because of the ability to detect these amidopalladium alkene complexes, we were able to probe the effect of the steric and electronic properties of the amido complex and the alkene reactant on the elementary migratory insertion step. Future work will focus on expanding the scope of insertions of alkenes into metal−heteroatom bonds and developing new palladium-catalyzed reactions that involve insertions of alkenes into metal−nitrogen bonds.

■ ASSOCIATED CONTENT

Supporting Information. Experimental procedures, characterization of complexes, insertion products, and computational details. This material is available free of charge via the Internet at http://pubs.acs.org.

■ AUTHOR INFORMATION

Corresponding Author
jhartwig@illinois.edu

■ ACKNOWLEDGMENT

We thank the Department of Energy for support, Johnson-Matthey for the donation of $Pd(OAc)_2$, Danielle Gray for collection of X-ray data, Dale Pahls for his assistance with the computations, and Prof. William D. Jones for assistance with kinetic simulations.

■ REFERENCES

(1) Grubbs, R. H.; Coates, G. W. *Acc. Chem. Res.* **1996**, *29*, 85.
(2) Ittel, S. D.; Johnson, L. K.; Brookhart, M. *Chem. Rev.* **2000**, *100*, 1169.
(3) Gibson, V. C.; Spitzmesser, S. K. *Chem. Rev.* **2003**, *103*, 283.
(4) Mecking, S. *Angew. Chem., Int. Ed.* **2001**, *40*, 534.
(5) Thalji, R. K.; Ahrendt, K. A.; Bergman, R. G.; Ellman, J. A. *J. Am. Chem. Soc.* **2001**, *123*, 9692.
(6) Tan, K. L.; Bergman, R. G.; Ellman, J. A. *J. Am. Chem. Soc.* **2002**, *124*, 13964.
(7) Periana, R. A.; Liu, X. Y.; Bhalla, G. *Chem. Commun.* **2002**, 3000.
(8) Oxgaard, J.; Periana, R. A.; Goddard, W. A. *J. Am. Chem. Soc.* **2004**, *126*, 11658.
(9) Lail, M.; Bell, C. M.; Conner, D.; Cundari, T. R.; Gunnoe, T. B.; Petersen, J. L. *Organometallics* **2004**, *23*, 5007.
(10) Nakao, Y.; Hirata, Y.; Hiyama, T. *J. Am. Chem. Soc.* **2006**, *128*, 7420.
(11) Nakao, Y.; Ebata, S.; Yada, A.; Hiyama, T.; Ikawa, M.; Ogoshi, S. *J. Am. Chem. Soc.* **2008**, *130*, 12874.
(12) Nakao, Y.; Idei, H.; Kanyiva, K. S.; Hiyama, T. *J. Am. Chem. Soc.* **2009**, *131*, 5070.
(13) Watson, M. P.; Jacobsen, E. N. *J. Am. Chem. Soc.* **2008**, *130*, 12594.
(14) Beletskaya, I. P.; Cheprakov, A. V. *Chem Rev* **2000**, *100*, 3009.
(15) Amatore, C.; Jutand, A. *Acc. Chem. Res.* **2000**, *33*, 314.
(16) Heck, R. F. *Acc. Chem. Res.* **1969**, *2*, 10.
(17) Heck, R. F. *Acc. Chem. Res.* **1979**, *12*, 146.
(18) Hartwig, J. F. *Organotransition metal chemistry: from bonding to catalysis*; University Science Books: Sausalito, Calif., 2010.
(19) Casalnuovo, A. L.; Calabrese, J. C.; Milstein, D. *J. Am. Chem. Soc.* **1988**, *110*, 6738.
(20) Cowan, R. L.; Trogler, W. C. *Organometallics* **1987**, *6*, 2451.
(21) Villanueva, L. A.; Abboud, K. A.; Boncella, J. M. *Organometallics* **1992**, *11*, 2963.
(22) Stubbert, B. D.; Marks, T. J. *J. Am. Chem. Soc.* **2007**, *129*, 6149.
(23) Majumder, S.; Odom, A. L. *Organometallics* **2008**, *27*, 1174.
(24) Leitch, D. C.; Payne, P. R.; Dunbar, C. R.; Schafer, L. L. *J. Am. Chem. Soc.* **2009**, *131*, 18246.
(25) Gagne, M. R.; Stern, C. L.; Marks, T. J. *J. Am. Chem. Soc.* **1992**, *114*, 275.
(26) Gribkov, D. V.; Hultzsch, K. C. *Angew. Chem., Int. Ed.* **2004**, *43*, 5542.
(27) Neukom, J. D.; Perch, N. S.; Wolfe, J. P. *J. Am. Chem. Soc.* **2010**, *132*, 6276.
(28) Neukom, J. D.; Perch, N. S.; Wolfe, J. P. *Organometallics* **2011**, *30*, 1269.
(29) Zhao, P. J.; Krug, C.; Hartwig, J. F. *J. Am. Chem. Soc.* **2005**, *127*, 12066.
(30) Nakhla, J. S.; Kampf, J. W.; Wolfe, J. P. *J. Am. Chem. Soc.* **2006**, *128*, 2893.
(31) Ney, J. E.; Wolfe, J. P. *J. Am. Chem. Soc.* **2005**, *127*, 8644.
(32) Mai, D. N.; Wolfe, J. P. *J. Am. Chem. Soc.* **2010**, *132*, 12157.
(33) Neukom, J. D.; Aquino, A. S.; Wolfe, J. P. *Org. Lett.* **2011**, *13*, 2196.
(34) Schultz, D. M.; Wolfe, J. P. *Org. Lett.* **2011**, *13*, 2962.
(35) Kotov, V.; Scarborough, C. C.; Stahl, S. S. *Inorg. Chem.* **2007**, *46*, 1910.
(36) Liu, G. S.; Stahl, S. S. *J. Am. Chem. Soc.* **2007**, *129*, 6328.
(37) Liu, G. S.; Yin, G. Y.; Wu, L. *Angew. Chem., Int. Ed.* **2008**, *47*, 4733.
(38) Liu, G. S.; Stahl, S. S. *J. Am. Chem. Soc.* **2006**, *128*, 7179.
(39) Muniz, K.; Hovelmann, C. H.; Streuff, J. *J. Am. Chem. Soc.* **2008**, *130*, 763.
(40) Helaja, J.; Gottlich, R. *Chem. Commun.* **2002**, 720.
(41) Tsutsui, H.; Narasaka, K. *Chem. Lett.* **1999**, 45.
(42) Ye, X. A.; Liu, G. S.; Popp, B. V.; Stahl, S. S. *J. Org. Chem.* **2011**, *76*, 1031.
(43) Hanley, P. S.; Markovic, D.; Hartwig, J. F. *J. Am. Chem. Soc.* **2010**, *132*, 6302.
(44) Although square-planar complexes typically undergo ligand exchange by associative processes, the direct observation of the equilibrium for dissociation of THF suggests that complex **2a** equilibrates with ethylene by a dissociative process.
(45) The approxiate observed rate contant was determined by plotting the decay of the concentration of the ethylene adduct **8** vs time and fitting the curve to an exponential decay. A good fit was observed, but the decay of **8** is not precisely first-order due to the presence of a small amount of dimer **4a**. The order of the reaction is not an integer value, and the observed rate constant for the decay of the concentration of **8** changes over the course of the reaction. A more detailed treatment of the data, including kinetic simulations, are presented later in this section and rigorously determine the rate constant for the insertion step.
(46) Barshop, B. A.; Wrenn, R. F.; Frieden, C. *Anal. Biochem.* **1983**, *130*, 134.

(47) Zimmerle, C. T.; Frieden, C. *Biochem. J.* **1989**, *258*, 381.
(48) All calculations were carried out with the Gaussian 09 program: Frisch, M. J.; *Gaussian 09,* revision A.1; Gaussian Inc.: Wallingford, CT, 2009. See the Supporting Information of the full reference.
(49) Roy, L. E.; Hay, P. J.; Martin, R. L. *J. Chem. Theory Comput.* **2008**, *4*, 1029.
(50) Ariafard, A.; Hyland, C. J. T.; Canty, A. J.; Sharma, M.; Brookes, N. J.; Yates, B. F. *Inorg. Chem.* **2010**, *49*, 11249.
(51) Bercaw, J. E.; Chen, G. S.; Labinger, J. A.; Lin, B. L. *Organometallics* **2010**, *29*, 4354.
(52) Ledford, J.; Shultz, C. S.; Gates, D. P.; White, P. S.; DeSimone, J. M.; Brookhart, M. *Organometallics* **2001**, *20*, 5266.
(53) Burger, B. J.; Santarsiero, B. D.; Trimmer, M. S.; Bercaw, J. E. *J. Am. Chem. Soc.* **1988**, *110*, 3134.
(54) Faller, J. W.; Chase, K. J. *Organometallics* **1995**, *14*, 1592.
(55) Malinoski, J. M.; White, P. S.; Brookhart, M. *Organometallics* **2003**, *22*, 621.
(56) Wang, L.; Flood, T. C. *J. Am. Chem. Soc.* **1992**, *114*, 3169.
(57) Rix, F. C.; Brookhart, M. *J. Am. Chem. Soc.* **1995**, *117*, 1137.
(58) Brookhart, M.; Volpe, A. F.; Lincoln, D. M.; Horvath, I. T.; Millar, J. M. *J. Am. Chem. Soc.* **1990**, *112*, 5634.
(59) Malinoski, J. M.; Brookhart, M. *Organometallics* **2003**, *22*, 5324.
(60) Chan, M. S. W.; Deng, L. Q.; Ziegler, T. *Organometallics* **2000**, *19*, 2741.
(61) Motta, A.; Lanza, G.; Fragala, I. L.; Marks, T. J. *Organometallics* **2004**, *23*, 4097.
(62) Marks and co-workers have studied the insertion step computationally and found a free energy of barrier $\Delta G^{\ddagger}$ = 12.5 kcal/mol (see ref 61). However, the reaction was conducted above room temperature. Thus, this free energy is calculated incorrectly, or migratory insertion is not the turnover limiting step.
(63) The cyclizations catalyzed by cationic zirconocene and titanocene complexes in ref 26 occur under similar conditions, but the turnover-limiting step in the catalytic process was not determined.
(64) Huffman, J. C.; Moloy, K. G.; Marsella, J. A.; Caulton, K. G. *J. Am. Chem. Soc.* **1980**, *102*, 3009.
(65) Schock, L. E.; Marks, T. J. *J. Am. Chem. Soc.* **1988**, *110*, 7701.
(66) To assess independently the potential accumulation of a styrene amido complex, we compared the relative rates for reactions of **2a** with two vinylarenes in separate reactions with the ratio of products from the reaction of **2a** with two vinylarenes together. In the absence of the accumulation of an amidopalladium vinylarene complex as an intermediate, one would expect the reaction with the two vinylarenes together to form about a 2:1 ratio of (*E*)-*N*-phenyl-*N*-((3-methoxy)styryl)aniline to (*E*)-*N*-phenyl-*N*-((4-methyl)styryl)aniline. If a vinylarene complex accumulates, this ratio would likely be different and be skewed toward the complex that forms the more stable adduct. In the event, the reaction of **2a** with 5 equiv of 4-methylsytrene and 5 equiv of 3-methoxysytrene generated enamine products in a total yield 60% yield consisting of a ~2:1 ratio of (*E*)-*N*-phenyl-*N*-(3-methoxy)styryl)aniline to (*E*)-*N*-phenyl-*N*-((3-methyl)styryl)aniline. This experiment corroborates the lack of accumulation of a stable amidopalladium vinylarene complex determined by the lack of a change in the NMR spectroscopic signals of **2a** upon addition of styrene.
(67) Ban, E.; Hughes, R. P.; Powell, J. *J. Organomet. Chem.* **1974**, *69*, 455.
(68) Miki, K.; Shiotani, O.; Kai, Y.; Kasai, N.; Kanatani, H.; Kurosawa, H. *Organometallics* **1983**, *2*, 585.
(69) Rix, F. C.; Brookhart, M.; White, P. S. *J. Am. Chem. Soc.* **1996**, *118*, 2436.
(70) Halpern, J.; Okamoto, T. *Inorg. Chim. Acta* **1984**, *89*, L53.
(71) Doherty, N. M.; Bercaw, J. E. *J. Am. Chem. Soc.* **1985**, *107*, 2670.